

# Online recursive estimation of remaining life using ultrasonic measurements

Dheeraj S Singh<sup>1</sup>, Shalabh Gupta<sup>2</sup> and Asok Ray<sup>1</sup>

## Abstract

This article addresses diagnosis and prognosis of evolving fatigue crack damage in polycrystalline alloy structures. It presents a statistically inspired recursive method for *in situ* estimation of the remaining useful life in machinery components, based on real-time measurements. The underlying algorithm is built upon (a) symbolic dynamic filtering of (online) ultrasonic sensor data and (b) Karhunen–Loëve decomposition of optical measurements for (off-line) construction of a stochastic model of fatigue crack propagation. The proposed method has been experimentally validated on a computer-instrumented and computer-controlled fatigue test apparatus for estimation of crack damage and prediction of the remaining useful life in test specimens, made of 7075-T6 aluminum alloys.

## Keywords

fatigue crack propagation, remaining useful life estimation, symbolic dynamic filtering

## Introduction

Fatigue damage is one of the most commonly encountered sources of structural degradation in aerospace, mechanical, and petrochemical systems.<sup>1</sup> Numerous fatigue damage monitoring techniques have been developed based on different sensing devices (e.g. ultrasonic, acoustic emission, and eddy current).<sup>2–4</sup> For example, Gupta and Ray<sup>5</sup> proposed an ultrasonic data-driven technique for early detection of incipient faults as well as real-time estimation of remaining fatigue life in polycrystalline alloys.

The work, reported in this article, presents formulation and experimental validation of an online method for fatigue crack damage estimation and remaining useful life prediction in polycrystalline alloy structures. The underlying algorithm is built upon symbolic dynamic filtering (SDF)<sup>6</sup> of ultrasonic data (that are sensed online) and (off-line) Karhunen–Loëve (K–L) decomposition of optical measurements of crack propagation.<sup>7</sup> In this context, major contributions of this article are as follows:

- Information fusion from ultrasonic and optical measurements of fatigue crack evolution for recursive damage estimation and remaining useful life prediction.

- K–L decomposition of stochastic optical information on crack length propagation to generate a single damage parameter that governs the damage propagation behavior.
- Construction of a recursive life estimation algorithm, in contrast to the nonrecursive method reported earlier.<sup>5</sup>
- Experimental validation of the recursive life estimation procedure on a fatigue test apparatus for polycrystalline alloy specimens.

The article is organized into six sections including the present one. “Details of Experimental Procedure” section describes the experimental apparatus and procedure employed for verification of the proposed life estimation technique. “SDF” section reviews SDF and summarizes the steps used for computation of the

<sup>1</sup>Department of Mechanical Engineering, The Pennsylvania State University, University Park, PA, USA

<sup>2</sup>Department of Electrical and Computer Engineering, University of Connecticut, Storrs, CT, USA

## Corresponding author:

Asok Ray, Department of Mechanical Engineering, The Pennsylvania State University, University Park, PA 16802, USA.

Email: [axr2@psu.edu](mailto:axr2@psu.edu)

evolving anomaly measure. “K–L Decomposition” section describes different steps used for K–L decomposition of test data. The proposed method of recursively estimating the damage parameter from observed anomaly measure is discussed in “Recursive Estimation of Remaining Useful Life” section. Subsequently, “Results and Discussions” section discusses the results obtained from application of the proposed algorithm on the test data collected from the laboratory apparatus. The article is concluded in “Summary, Conclusion, and Future Work” section along with recommendations for future research.

## Details of experimental procedure

This section presents the details of the test apparatus that experimentally validates the proposed fatigue life estimation procedure. It also briefly describes the specimen details and the test procedure employed.

### Test apparatus

The test apparatus, shown in Figure 1, consists of the following three major components:

1. *Fatigue testing machine*: It is a special-purpose uniaxial testing machine, which is operated on a computer-instrumented system under load control or strain control at speeds up to 12.5 Hz. The test specimens are subjected to tensile–tensile cyclic loading by a hydraulic servo system under the regulation of computer-controlled electrohydraulic valves.
2. *Traveling optical microscope*: It provides direct measurements of the visible part of a crack. The resolution of the optical microscope is about  $2\text{ }\mu\text{m}$  at a working distance of 10–35 cm, and the images are taken at a magnification of  $75\times$ . The growth of the crack is monitored continuously by the microscope, which takes the images of the surface of the specimen at regular intervals.
3. *Ultrasonic flaw detection system*: This system is triggered to send pulses to ultrasonic transducer and receive the ultrasonic signal either from same transducer in the pulse-echo mode or from other transducers in the through mode. The ultrasonic system is triggered, when the load applied at a specimen reaches a certain limit.

### Specimen details

As shown in Figure 1, side-notched 7075-T6 aluminum specimens have been used on the apparatus for test and validation of the derived diagnosis, prognosis, and life

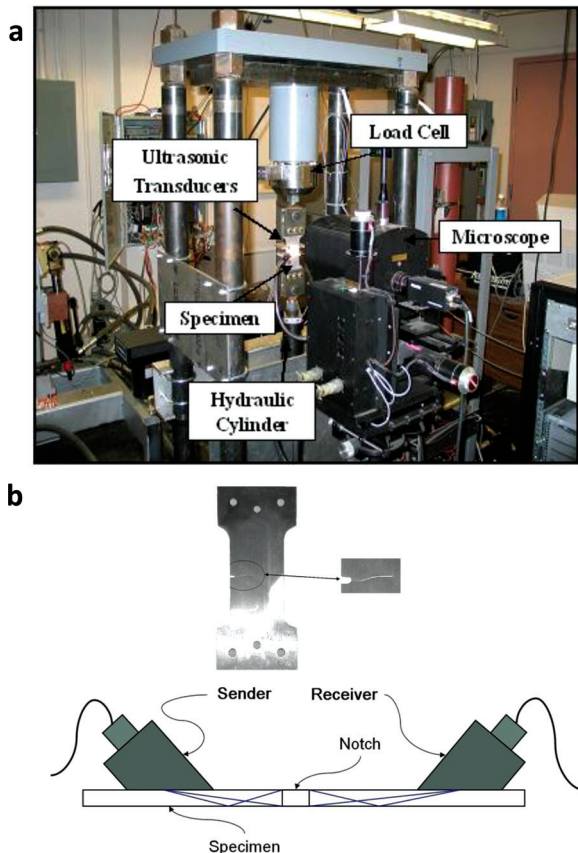


**Figure 1.** Computer-instrumented apparatus for fatigue testing and schematic of ultrasonic sensors on a test specimen: (a) fatigue testing apparatus and (b) specimen and mounting of the ultrasonic sensors.

estimation algorithms. Typical specimens are 3 mm thick and 50 mm wide and have a slot of  $1.58\text{ mm}\times 4.57\text{ mm}$  on one side. The notch is made to increase the stress concentration factor that ensures crack initiation and propagation at the notch end. The test specimens have been subjected to sinusoidal loading under tension–tension mode (i.e. with a constant positive offset) at a frequency of 12.5 Hz. A constant bias offset is provided in the load cycling to ensure that the specimen is always under tension.

### Test procedure

The fatigue tests have been conducted at a constant amplitude sinusoidal load for low-to-medium cycle fatigue, where the maximum and minimum loads are kept constant at 87 and 4.85 MPa, respectively, so that the resulting stress amplitude at the crack tip is sufficiently high to observe the elastoplastic behavior in the specimens under cyclic loading. A significant amount of internal damage caused by multiple small cracks,

dislocations, and microstructural defects alters the ultrasonic impedance, which causes signal distortion and attenuation at the receiver end. It is assumed that at the onset of the crack propagation phase, a dominant crack is created (possibly) due to coalescence of several small cracks that have gradually evolved during the crack initiation phase. In the analysis and its experimental validation, as reported in this article, the crack damage is defined in terms of the length of this dominant crack that is recorded by the optical microscope. However, the ultrasonic signals measure the resulting influence of the dominant crack as well as other (possibly small) cracks.

The optical images are collected autonomously at every 200 cycles by the optical microscope that is always focused at the crack tip. After the crack becomes visible by the microscope, the crack length is measured and recorded at every 200 cycles. Ultrasonic waves with a frequency of 5 MHz are triggered at each peak of the sinusoidal load to generate data points in each cycle. Since the ultrasonic frequency is much higher than the load frequency, data acquisition is conducted for a very short interval in the time scale of load cycling. Therefore, it is implied that ultrasonic data are collected around the peak of each sinusoidal load cycle, where the stress is maximum and the crack is open causing maximum attenuation of the ultrasonic waves. The slow-time epochs for data analysis are chosen to be 1000 load cycles (i.e.  $\sim 80$  s) apart. Tests were conducted for 35 similarly manufactured specimens; for each specimen, data were collected at 30 consecutive time epochs after the first appearance of a crack as detected by the optical microscope.

## Symbolic Dynamic Filtering (SDF)

While the theory of symbolic dynamic filtering (SDF) has been reported in the literature,<sup>6,8</sup> the underlying concept is succinctly presented here for completeness of the article.

A key step in an SDF analysis is to represent time series data, generated from a dynamical system, as a symbol sequence. Let  $\Theta \in R^n$  be a compact (i.e. closed and bounded) region, within which the trajectory of the dynamical system is circumscribed. The region  $\Theta$  is partitioned into a finite number of (mutually exclusive and exhaustive) cells, so as to obtain a coordinate grid. A cell, visited by the trajectory, is denoted as a random variable taking symbol values from a predefined alphabet  $\Sigma$ .

Let an orbit of the dynamical system be described as  $\{y_0, y_1, \dots, y_k, \dots\}$  with  $y_i \in \Theta$ , which passes through or touches one of the cells of the partition. The symbol sequence is denoted as  $\{\sigma_0, \sigma_1, \dots, \sigma_k, \dots\}$ , where each

symbol  $\sigma_i$  belongs to the (finite) alphabet  $\Sigma$ . Thus, symbolic dynamics could be viewed as coarse graining of the data space, which is subjected to (possible) loss of information resulting from granular imprecision of the partitioning process. However, the essential robust features are preserved in the symbol sequences through an appropriate partitioning of the region  $\Theta$ .

Several partitioning techniques have been reported in the literature for symbol generation. These techniques are primarily based on symbolic false nearest neighbors (SFNNs),<sup>9</sup> which may become cumbersome and extremely computation intensive if the data set is contaminated by noise. As an alternative, the time series data can be partitioned for symbol sequence generation using either the uniform or the maximum entropy partitioning.<sup>10</sup> For the analysis of noise-corrupted data, prior to partitioning, the time series data may be processed using an appropriately chosen wavelet transform.<sup>8,11</sup>

Once the symbol sequence is generated, the next step is construction of probabilistic finite state automata (PFSA) for modeling the statistical dependencies among the occurrences of symbols. The symbolic sequence is modeled as a  $D$ -Markov process, where the likelihood of a future symbol depends only on the previous  $D$  symbols.<sup>6</sup> This assumption leads to the construction of PFSA, wherein the state transition probabilities depict the conditional dependencies between symbols. The state probability vector  $\mathbf{q}$ , which is derived from the PFSA at a given time epoch by frequency counting of its states, serves as a statistical information pattern of the underlying process.<sup>6,8,12</sup> In this way, the state probability vectors are computed at different time epochs, where the damage slowly evolves. Subsequently, a scalar anomaly measure  $\mu_n$  is defined as

$$\mu_n = d(\mathbf{q}_n, \mathbf{q}_0) \quad (1)$$

where  $\mathbf{q}_n$  and  $\mathbf{q}_0$  are the information patterns obtained by an SDF analysis at the epochs  $t_n$  (current time) and  $t_0$  (nominal condition), respectively, and  $d$  is an appropriate distance function.<sup>8,5</sup> In this article, the angular distance between two vectors has been chosen as the distance function<sup>6</sup>:

$$d(\mathbf{q}_n, \mathbf{q}_0) \triangleq \cos^{-1} \left( \frac{\langle \mathbf{q}_n, \mathbf{q}_0 \rangle}{\|\mathbf{q}_n\|_2 \|\mathbf{q}_0\|_2} \right) \quad (2)$$

where  $\langle \bullet, \star \rangle$  is the inner product of the pattern vectors  $\bullet$  and  $\star$ , and  $\|\bullet\|_2$  is the Euclidean norm of the pattern vector  $\bullet$ . In essence, the ultrasonic signals are analyzed by SDF to yield the anomaly measure  $\mu_n$  at each discrete time epoch  $n$  via equations (1) and (2). The details of the procedure are described in Ref. 12.

### Remark

The algorithms of an SDF analysis have been experimentally validated for real-time execution in diverse applications, including electronic circuits,<sup>6</sup> fatigue damage monitoring in polycrystalline alloys,<sup>5,8</sup> and robot signature analysis.<sup>11</sup> An important aspect of using SDF is that it makes relative measures of anomalies, as shown in equation (2), instead of making evaluations in an absolute sense. This is particularly advantageous for ultrasonic (UT) measurements, where UT wedges may introduce different reference patterns  $\mathbf{q}_0$  for individual samples.

### Karhunen–Loève (K–L) Decomposition

This section presents the analysis of fatigue crack data, obtained (off-line) using an optical microscope, via K–L decomposition.<sup>7</sup> A nondimensional stochastic measure  $\psi$  of fatigue crack damage is defined as

$$\psi_t(\zeta, t_0) \triangleq \frac{c_t(\zeta)}{c_{t_0}(\zeta)} \quad \text{for } t \geq t_0 \quad (3)$$

where  $\zeta$  is a sample point representing randomness,  $c_t(\zeta)$  is the crack length at time  $t$ , and  $c_{t_0}(\zeta) \sim 500 \mu\text{m}$  is the crack length at the initial time  $t_0$ . Since time series of crack length measurements are recorded at only finitely many ( $\ell$ ) time epochs during the entire loading experiment for each sample (i.e. test specimen), the stochastic process  $\psi_t(\zeta, t_0)$  reduces to an  $l$ -dimensional random vector denoted as  $\Psi^D(\zeta)$ , whose  $(\ell \times 1)$  mean  $m_\Psi^D$  and  $(\ell \times \ell)$  covariance matrix  $C_{\Psi\Psi}^D$  are defined as

$$\begin{aligned} m_\Psi^D &\triangleq E[\Psi^D(\zeta)] \\ C_{\Psi\Psi}^D &\triangleq E[(\Psi^D(\zeta) - m_\Psi^D)(\Psi^D(\zeta) - m_\Psi^D)^T] \end{aligned} \quad (4)$$

(Note: As stated at the end of “Test Procedure” section, number of samples = 35, that is,  $\zeta=1, \dots, 35$  and, for each sample  $\zeta$ , number of time epochs  $\ell=30$  at which time series of crack length measurements are recorded and ultrasonic data are collected.)

Assuming that the experimental data are collected at sufficiently close intervals,  $C_{\Psi\Psi}^D$  contains pertinent information of the crack damage process. Let the  $\ell$  eigenvalues of  $C_{\Psi\Psi}^D$  be ordered as  $\lambda_1 \geq \lambda_2 \geq \dots \geq \lambda_\ell$ , with the corresponding eigenvectors  $\varphi^1, \varphi^2, \dots, \varphi^\ell$  that form an orthonormal basis of the Euclidean space  $R^\ell$  for signal decomposition.

The K–L decomposition also ensures that the  $\ell$  random coefficients of the basis vectors are statistically orthogonal (i.e. zero mean and mutually uncorrelated).<sup>13–15</sup> These random coefficients denoted as a random vector  $\{x_1(\zeta)x_2(\zeta)\dots x_\ell(\zeta)\}$  with a covariance matrix  $C_{XX} = \text{diag}(\lambda_1, \lambda_2, \dots, \lambda_\ell)$ . The decomposition of

discretized damage process is obtained in the mean square (MS) sense as

$$\begin{aligned} \Psi^D(\zeta) &\stackrel{\text{ms}}{=} m_\Psi^D + \sum_{j=1}^{\ell} x_j(\zeta) \varphi^j \\ &\Rightarrow \Psi^D(\zeta) \stackrel{\text{ms}}{=} \underbrace{m_\Psi^D + x_1(\zeta) \varphi^1}_{\text{Principal part}} + \underbrace{\sum_{j=2}^{\ell} x_j(\zeta) \varphi^j}_{\text{Residual part}} \end{aligned} \quad (5)$$

As shown in equation (5), the crack damage process is expressed as the sum of the principal and residual parts that are mutually statistically orthogonal. It is shown in an earlier publication<sup>7</sup> that the statistics of fatigue crack damage are dominated by the random coefficients corresponding to the principal eigenvector  $\varphi^1$ , associated with the largest eigenvalue  $\lambda_1$ . Along this line, the principal part is considered as the estimated damage and the residual part as the estimation error. This is in agreement with the K–L analysis of the experimental test data, where the MS error is determined as

$$\varepsilon_{\text{rms}}^2 = \frac{\sum_{j=2}^{\ell} \lambda_j}{\sum_{j=1}^{\ell} \lambda_j} \quad (6)$$

which shows that MS estimation error  $\varepsilon_{\text{rms}}^2 \approx 0.017$ . Thus, the random coefficient of the principal eigenvector approximates the process of damage evolution and is denoted by  $\Omega(\zeta) \triangleq x_1(\zeta)$ . By neglecting the zero-mean residual part with a small variance in equation (5), the damage is approximated as

$$\Psi^D(\zeta) \approx m_\Psi^D + \Omega(\zeta) \varphi^1 \quad (7)$$

The (random) damage parameter  $\Omega(\zeta)$  is evaluated for each sample point  $\zeta$  from experimental data as the average slope of the plot in the graph generated with  $(\Psi^D(\zeta) - m_\Psi^D)$  as the ordinate and the principal eigenvector  $\varphi^1$  as the abscissa. Here,  $\Psi^D(\zeta)$  is the damage vector of the sample  $\zeta$  and  $m_\Psi^D$  the mean vector obtained from the damage vectors of all samples. The computed values of  $\Omega(\zeta)$  are used to model a normal probability distribution fit as shown in Figure 2, where the goodness of fit exceeds 10% significance level in the  $\chi^2$  sense.<sup>16</sup> This probability distribution is used as the prior knowledge  $p_0(\Omega)$  for recursive identification of the distribution  $p_n(\Omega)$  in the remaining useful life estimation procedure described in “Recursive Estimation of Remaining Useful Life” section.

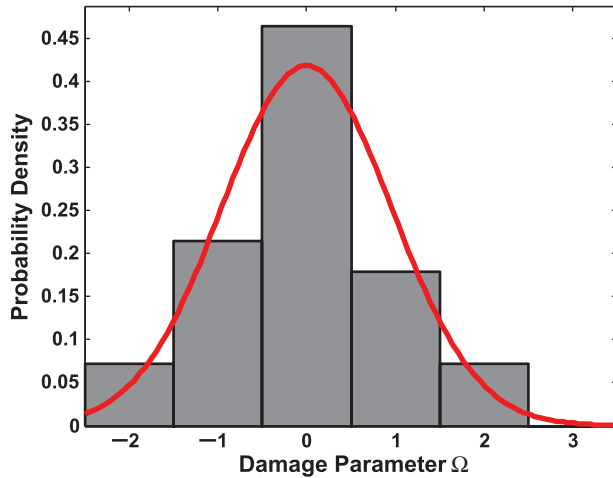


**Figure 2.** Normal distribution (mean  $\mu=0$  and variance  $\sigma^2 \approx 0.95$ ) fit of the damage parameter  $\Omega$  at 0 kilocycles.

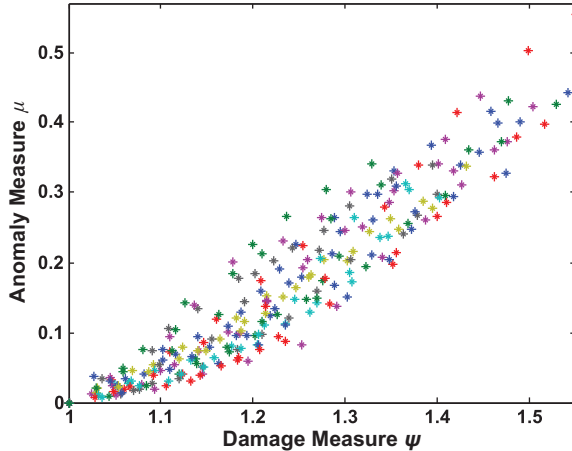


**Figure 3.** Statistical data of fatigue damage parameters. This data set is generated using (a) the stochastic data of crack length versus time obtained from the optical microscope and (b) the stochastic data of anomaly measure versus time generated from the SDF analysis of the corresponding ultrasonic data sets. The anomaly measure  $\{\mu_k\}$  and damage measure  $\{\psi_k\}$  are recorded and plotted at each time epoch  $k$  for each sample.

### Recursive estimation of remaining useful life

This section presents an online recursive method to compute a probability distribution of the remaining useful life. Since it is difficult to obtain optical microscope data in real time, this article utilizes in situ ultrasonic measurements for recursive estimation of remaining useful life. As stated earlier in “SDF” section, the ultrasonic signals are analyzed by SDF to yield the anomaly measure  $\mu_n$  at each discrete time epoch  $n$  (equations (1) and (2)).

Following equation (7), the scalar form of the evolving damage at a discrete time epoch  $n$  is modeled as

$$\psi_n(\zeta) \approx m_{\psi_n} + \Omega(\zeta)\varphi_n^1 \quad (8)$$

Since input loading is uniform across all samples, the anomaly measure in equation (1) is a function of the damage measure  $\psi_n(\zeta)$  with additive noise due to variability in ultrasonic sensing. Therefore, for recursive estimation of the random parameter  $\Omega(\zeta)$  based on the history of anomaly measure, its conditional probability distribution is defined such that

$$p_n(\Omega) \stackrel{\Delta}{=} p(\Omega|\mu_n, \mu_{n-1}, \dots, \mu_1, \mu_0) \quad (9)$$

where  $p_n(\Omega)$  is updated after  $\mu_n$  is computed online.

To start the recursive process,  $p_0(\Omega)$  is obtained from the probability distribution fitted in Figure 2. Since the measurement  $\mu_n$  is assumed to be conditionally independent of the collection of all previous measurements  $\mu_1, \mu_2, \dots, \mu_{n-1}$ , that is,  $p(\mu_n|\Omega, \mu_{n-1}, \dots, \mu_1, \mu_0) = p(\mu_n|\Omega)$ , it follows from Bayesian principles that

$$p_n(\Omega) = \frac{p(\mu_n|\Omega)p_{n-1}(\Omega)}{\int d\Omega p(\mu_n|\Omega)p_{n-1}(\Omega)} \quad (10)$$

where the initial distribution  $p_0(\Omega)$  is obtained as described at the end of “K–L Decomposition” section (see also Figure 2). In equation (10),  $p_{n-1}(\Omega)$  is the posterior probability distribution after  $(n-1)$ th measurement and is recursively updated after  $n$ th anomaly measure  $\mu_n$  is computed online.

The a priori conditional probability density  $p(\mu_n|\Omega)$  is identified from the statistical data in Figure 3, where the anomaly measure  $\{\mu_k\}$  and damage measure  $\{\psi_k\}$  are recorded and plotted at each time epoch for each sample. This data set is generated using (a) the stochastic data of crack length propagation versus time obtained from the optical microscope and (b) the stochastic data of anomaly measure profiles versus time generated from the SDF analysis of the corresponding ultrasonic data sets. Variations in anomaly measure  $\mu$  at a given damage measure  $\psi$ , which is in turn related to the damage parameter  $\Omega$ , are subjected to measurement noise and are fitted (off-line) with a lognormal distribution,<sup>7</sup> where the goodness of fit is around 10% significance level in the  $\chi^2$  sense<sup>16</sup>; this yields the a priori distribution  $p(\mu|\Omega)$  in equation (10).

In the real-time operation, the objective is to compute  $p(\mu_n|\Omega)$  for the in situ measured value of  $\mu_n$  at time epoch  $n$ . Thus, for each realization  $\Omega(\zeta)$ , the corresponding damage measure  $\psi_n(\zeta)$  at  $n$ th time epoch is obtained from equation (8). Subsequently, the conditional probability  $p(\mu_n|\Omega)$  is obtained from the

distribution of  $\mu$  generated off-line, which in turn yields  $p_n(\Omega)$  from  $p_{n-1}(\Omega)$  (see equation (10)).

The updated probability distribution  $p_n(\Omega)$  is then used to estimate the remaining useful life. The total life of a sample is defined as the number of fatigue cycles taken to reach a critical value  $\psi_{crit}$  of the damage measure, after which the crack growth is expected to be very rapid and leads to complete breakage of the specimen within a few cycles. Thus, the estimation of remaining useful life is equivalent to computation of the number of cycles required to reach the critical value of damage measure. It is known that each sample  $\zeta$  takes a different fatigue damage propagation path. Since  $\Omega(\zeta)$  is a random variable that is constant for a given sample  $\zeta$ , the computed probability distribution  $p_n(\Omega)$  provides the probability distribution of different damage propagation paths (see equation (7)) that the current sample is taking.

For the test procedure at hand, the remaining useful life (i.e. the number of cycles left to reach the critical value of  $\psi$ ) of a certain sample at an epoch  $n$  is experimentally evaluated from the off-line crack propagation data. The remaining useful life  $\tau$  being statistically dependent on the damage parameter  $\Omega$ , the probability density  $q_n(\tau)$  is obtained from the probability density  $p_n(\Omega)$  based on the following model construction:  $q_n(\tau) \equiv p_n(\Omega)|d\Omega/d\tau|$ , that is,  $q_n(\tau)|d\tau| \equiv p_n(\Omega)|d\Omega|$ , implying that the probability increments are invariant under a smooth change of variables from the  $\Omega$  domain to the  $\tau$  domain.

Once the probability distribution of remaining useful life  $\tau$  is obtained, the pertinent statistical information is obtained. These statistical parameters are as follows:

1. Statistical mean of the remaining useful life  $m_\tau \stackrel{\Delta}{=} \int \tau q_n(\tau)d\tau$  and its statistical variance  $\sigma_\tau^2 \stackrel{\Delta}{=} \int \tau^2 q_n(\tau)d\tau$ .
2. Maximum likelihood estimate  $\hat{\tau}$  of the remaining useful life  $\tau$ , that is, where the probability distribution  $q_n(\tau)$  attains the maximum value. (Note:  $q_n(\tau)$  is non-Gaussian.)
3. The 95% confidence intervals for remaining useful life  $\tau$  having upper-bound  $\tilde{\tau}_U$  and lower-bound  $\tilde{\tau}_L$ .

## Results and discussions

This section presents the results of experimental validation of the recursive remaining useful life estimation method on the test apparatus described in “Details of Experimental Procedure” section. Before embarking on discussion of the test results, the steps involved in remaining useful life estimation are summarized in the following:

1. A set of stochastic data have been generated from 35 similarly manufactured test specimens. This set includes data collected from two different sensors at 30 consecutive time epochs for each specimen: (a) data of crack length propagation obtained from an optical microscope and (b) the corresponding ultrasonic data obtained from the receiver transducer. For each specimen  $\zeta$ , the optical crack length information is used to compute the damage measure  $\{\psi_n\}$  at discrete time epochs  $n$ , thus generating a random vector  $\Psi^D(\zeta)$  in equation (7). The corresponding ultrasonic data are analyzed using SDF to compute the anomaly measure  $\{\mu_n\}$  at the corresponding epochs  $n$  (see equations (1) and (2)).
2. The damage measure  $\psi$  is generated by K-L decomposition of optical data of crack length propagation (see “K-L Decomposition” section) to obtain the random damage parameter  $\Omega(\zeta)$  for each specimen. These data are fitted with a normal probability distribution. The fitted probability distribution is termed as the prior probability distribution of  $\Omega$  and is denoted by  $p_0(\Omega)$ .
3. Test experiments have been conducted to validate the recursive algorithm of remaining useful life estimation. At the start of a test experiment,  $p_0(\Omega)$  is used to generate probability distribution  $q_0(\tau)$  of remaining useful life. As the experimentation is continued and damage growth evolves in the test sample, new ultrasonic measurements are taken. Anomaly measure  $\mu_n$  is calculated by SDF of each ultrasonic measurement (see “SDF” section) recorded at time  $n$ . After such information is available, the probability distribution  $p_n(\Omega)$  is updated by equation (10) as explained in “Recursive Estimation of Remaining Useful Life” section. This equation uses statistical information available from Step 1 to calculate  $p(\mu_n|\Omega)$ .
4. Remaining useful life  $\tau(\zeta)$  of a sample  $\zeta$  is a random variable dependent on the damage parameter  $\Omega(\zeta)$ . Updated probability distribution  $p_n(\Omega)$  is recursively computed from the information generated in the earlier step to find the corresponding probability distribution of remaining useful life  $q_n(\tau)$ . Equation (7) is used to find the damage vector  $\Psi^D(\zeta)$  for each sample  $\zeta$ . Each element  $\psi_n(\zeta)$  of damage vector  $\Psi^D(\zeta)$  represents the value of damage measure at the time epoch  $n$ . Total life is defined as time  $t$  when damage measure  $\psi_t(\zeta)$  reaches the critical value  $\psi_{crit}$  that is taken to be 1.8 (by extension of the abscissa in Figure 3). Thus, the remaining useful life  $\tau(\zeta)$  is determined for each sample  $\zeta$  by interpolating damage vector  $\Psi^D(\zeta)$  between two consecutive epochs. Now, the

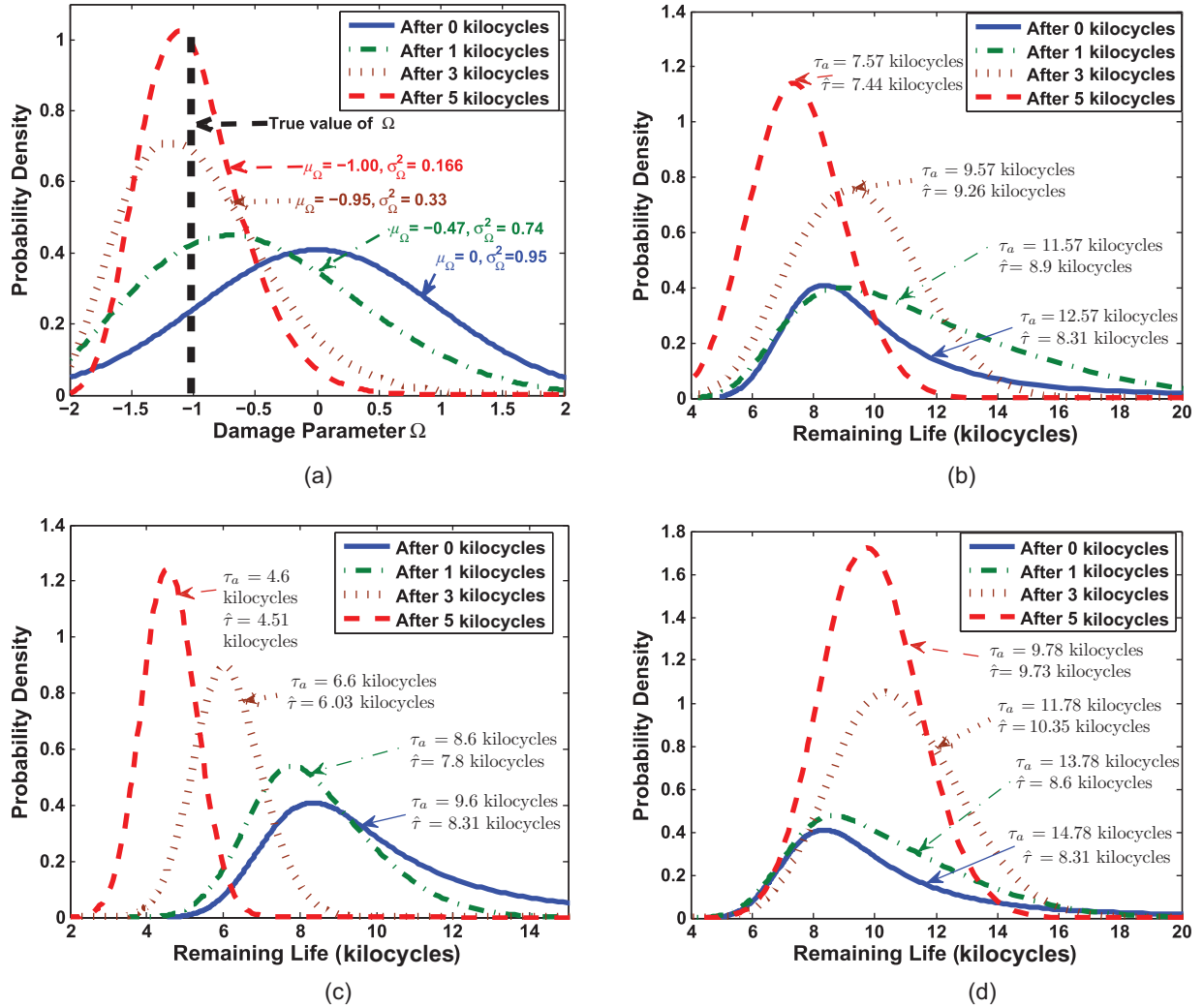


**Figure 4.** Recursive estimation of probability density functions (PDFs) of the parameter  $\Omega$  and the remaining useful life: (a) recursive estimation of for Sample 1, (b) recursive estimation of remaining useful life for Sample 1, (c) recursive estimation of remaining useful life for Sample 2, and (d) recursive estimation of remaining useful life for Sample 3. Three test examples are shown.  $\mu_{\Omega}$ : mean value of  $\Omega$ ;  $\sigma_{\Omega}^2$ : variance of  $\Omega$ ;  $\tau_a$ : true value of the remaining useful life;  $\hat{\tau}$ : maximum likelihood estimate.

- probability distribution  $q_n(\tau)$  of remaining useful life  $\tau$  is derived from  $p_n(\Omega)$  by change of variables.
5. Relevant statistical information is derived from  $q_n(\tau)$  as described in the last paragraph of “Recursive Estimation of Remaining Useful Life” section.

While experiments on test specimens have been conducted to validate the proposed life estimation algorithm, the results obtained from three typical experiments are now presented. Figure 4(a) shows the estimated (conditional) probability distributions of the random parameter  $\Omega$  at different time epochs. The ultrasonic signal recorded at the onset of crack propagation is taken as the reference signal, and the

corresponding anomaly measure is  $\mu_0 = 0$  (see equation (1)). The solid line indicates the initial probability distribution  $p_0(\Omega)$  that is known a priori, as shown in Figure 2. As subsequent ultrasonic measurements become available, the anomaly measures are computed using SDF to update the posterior probability density  $p_n(\Omega)$  according to equation (10). The remaining three curves in Figure 4(a) display the posterior probability distributions  $p_1(\Omega)$ ,  $p_3(\Omega)$ , and  $p_5(\Omega)$  at 1000, 3000, and 5000 cycles, respectively. The vertical dashed line at  $\Omega = -1$  represents the true value of the damage parameter  $\Omega$  for this sample, which is computed from the crack length data after completion of the experiment.

Each of Figure 4(b) to (d) presents four curves, representing the probability density function (PDF) of the

**Table I.** True and estimated remaining useful life ( $\tau$ ) values with corresponding anomaly measure for three test samples

Test sample	Observed $\mu$	$\tau_a$	$m_{\tau}$	$\sigma_{\tau}$	$\hat{\tau}$	$\tilde{\tau}_L$	$\tilde{\tau}_U$
1	0.0099207	11.5708	9.2535	2.7392	8.8893	3.8847	14.6223
	0.027221	10.5708	8.995	2.2966	9.9221	4.4936	13.4964
	0.041484	9.5708	8.5278	1.9746	9.2636	4.6576	12.398
	0.06175	8.5708	7.7111	1.6868	8.0897	4.4049	11.0173
	0.073062	7.5708	7.0058	1.4914	7.4444	4.0826	9.929
2	0.020483	8.6089	7.9015	1.4509	7.8007	5.477	11.0051
	0.045099	7.6089	6.8345	1.0597	6.8383	5.028	9.1007
	0.062375	6.6089	6.0214	0.88507	6.0301	4.6025	8.3813
	0.074748	5.6089	5.3331	0.79906	5.3468	3.9648	7.1007
	0.10181	4.6089	4.5384	0.71232	4.5179	3.3106	6.0335
3	0.012597	13.7813	9.0553	2.1973	8.6069	5.7203	13.8766
	0.01996	12.7813	9.818	2.2257	10.2636	6.1818	14.3494
	0.027909	11.7813	10.1846	2.0292	10.3532	7.0398	15.2387
	0.034661	10.7813	10.261	1.852	10.1906	7.3094	14.4821
	0.051231	9.7813	9.7185	1.6237	9.7327	7.0051	13.2387

$\mu$ : anomaly measure;  $\tau_a$ : true value of  $\tau$ ;  $\hat{\tau}$ : maximum likelihood estimate of  $\tau$ ;  $m_{\tau}$ : mean value of  $\tau$ ;  $\sigma_{\tau}$ : standard deviation of  $\tau$ ;  $\tilde{\tau}_U$ : upper bound of  $\tau$ ;  $\tilde{\tau}_L$ : lower bound of  $\tau$  (95% confidence interval).

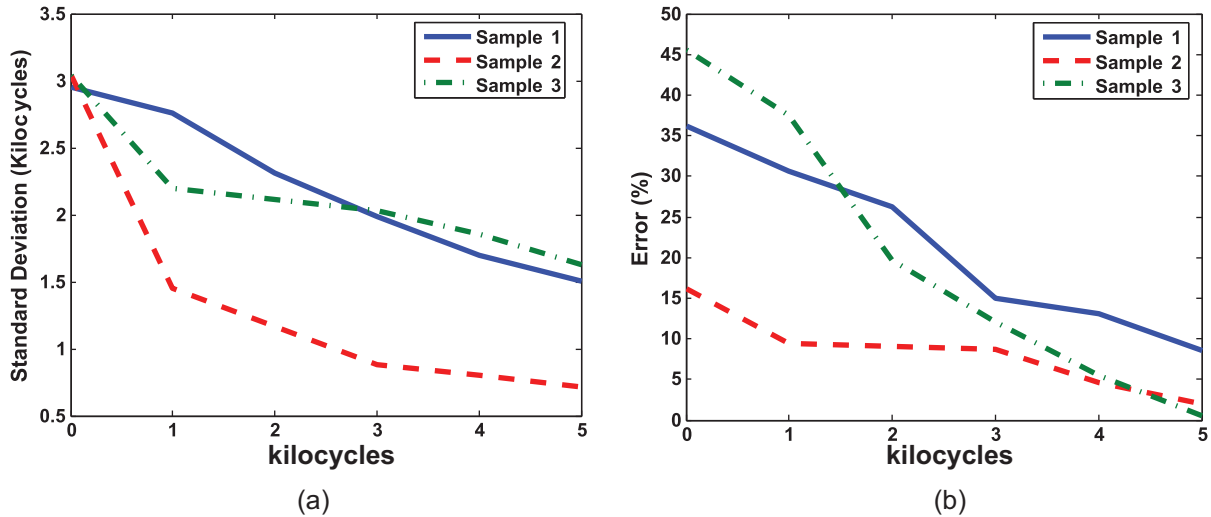


**Figure 5.** Results of remaining useful life estimation from test samples: (a) standard deviation ( $\sigma_{\tau}$ ) of remaining useful life for three samples and (b) percent error of remaining useful life for three samples.

remaining useful life ( $\tau$ ) at different stages during the experimentation for three different test specimens, respectively. Each plot is marked with the corresponding value of actual remaining useful life ( $\tau_a$ ) and the maximum likelihood estimate of remaining useful life ( $\hat{\tau}$ ). As the number of cycles increase, the variance of the estimated (conditional) PDF decreases; consequently, more information becomes available on how the specimen life is consumed as time progresses. The recursively generated probability densities are used to compute the expected value ( $m_{\tau}$ ), standard deviation ( $\sigma_{\tau}$ ), maximum likelihood estimate ( $\hat{\tau}$ ), and upper ( $\tilde{\tau}_U$ )

and lower ( $\tilde{\tau}_L$ ) bounds of 95% confidence interval of the remaining useful life. The estimated remaining useful life  $\hat{\tau}$  values are compared with those of the actual remaining useful life ( $\tau_a$ ) as shown in Table 1 for the three test specimens. It is evident from the experimental results in Table 1 as well as in Figure 5(a) and (b) for the three test specimens that as more measurements become available, both standard deviation and estimation error of the remaining useful life decrease consistently. Hence, it is concluded that the remaining useful life of the structural component can be more reliably estimated with the in situ ultrasonic measurements. For

example, this information on the remaining useful life estimate can be used in real-time life-extending control strategies<sup>17</sup> for timely prediction and mitigation of widespread damage and structural failures.

## Summary, conclusion, and future work

This article presents a data-driven statistical method for real-time estimation of the remaining useful life in polycrystalline alloy structures. The (online) ultrasonic signals and (off-line) optical measurements of crack propagation are analyzed for estimation of fatigue crack damage and statistical prediction of the remaining useful life. The proposed method is experimentally validated on a laboratory apparatus<sup>5</sup> for 7075-T6 aluminum specimens. This concept is potentially applicable for fault detection in dynamical systems with multiple sources of correlated faults.

The reported work is a preliminary step toward building a reliable instrumentation system for early detection of fatigue crack damage and real-time prediction of the remaining useful life in mechanical structures based on in situ ultrasonic sensors. For example, the information on current health status and remaining useful life could be used to update the decision and control laws of operation and maintenance to avert forthcoming failures and to enhance plant performance. To this end, application areas of the proposed method of remaining useful life prediction include life-extending control and resilient control in complex engineering systems.<sup>17</sup> While there are many research issues that need to be addressed, the following potential future tasks are envisioned:

- Estimation of multiple damage parameters under variable amplitude and random loading conditions.
- Remaining useful life prediction in the crack initiation regime based on changes in surface profile as a measure of fatigue damage.<sup>18</sup>

## References

1. Suresh S. *Fatigue of materials*. 2nd ed. Cambridge: Cambridge University Press, 1998.
2. Grondel S, Delebarre C, Assaad J, et al. Fatigue crack monitoring of riveted aluminium strap joints by lamb wave analysis and acoustic emission measurement techniques. *NDT & E Int* 2006; 35: 339–351.
3. Zilberstein V, Walrath K, Grundy D, et al. MWM eddy-current arrays for crack initiation and growth monitoring. *Int J Fatigue* 2003; 25: 1147–1155.
4. Shan Q and Dewhurst RJ. Surface-breaking fatigue crack detection using laser ultrasound. *Appl Phys Lett* 1993; 62(21): 2649–2651.
5. Gupta S and Ray A. Real-time fatigue life estimation in mechanical systems. *Meas Sci Technol* 2007; 18(7): 1947–1957.
6. Ray A. Symbolic dynamic analysis of complex systems for anomaly detection. *Signal Process* 2004; 84(7): 1115–1130.
7. Ray A. Stochastic measure of fatigue crack damage for health monitoring of ductile alloy structures. *Struct Health Monit* 2004; 3(3): 245–263.
8. Gupta S, Ray A and Keller E. Symbolic time series analysis of ultrasonic data for early detection of fatigue damage. *Mech Syst Signal Process* 2007; 21(2): 866–884.
9. Buhl M and Kennel M. Statistically relaxing to generating partitions for observed time-series data. *Phys Rev E* 2005; 71(4): 046213.
10. Rajagopalan V and Ray A. Symbolic time series analysis via wavelet-based partitioning. *Signal Process* 2006; 86(11): 3309–3320.
11. Jin X, Gupta S, Mukherjee K, et al. Wavelet-based feature extraction using probabilistic finite state automata for pattern classification. *Pattern Recognit* 2011; 44(7): 1343–1356.
12. Gupta S and Ray A. Symbolic dynamic filtering and data-driven pattern recognition. In: Zoeller EA (ed.) *Pattern recognition: theory and applications*. Hauppauge, NY: Nova Science Publishers, 2007, pp.17–71.
13. Fukunaga DP. *Statistical pattern recognition*. 2nd ed. Boston, MA: Academic Press, 1990.
14. Bishop CM. *Pattern recognition and machine learning (information science and statistics)*. Secaucus, NJ: Springer-Verlag, 2006.
15. Duda RO, Hart PE and Stork DG. *Pattern classification*. 2nd ed. New York: Wiley Interscience, 2001.
16. Brunk H. *An introduction to mathematical statistics*. 3rd ed. Lexington, MA: Xerox College Publishing, 1975.
17. Zhang H, Ray A and Phoha S. Hybrid life extending control of mechanical systems: experimental validation of the concept. *Automatica* 2000; 36(1): 23–36.
18. Singh DS, Gupta S and Ray A. Symbolic dynamic analysis of surface deformation during fatigue crack initiation. *Meas Sci Technol* 2010; 21(4): 043003(7pp.).